

AD-A100 007

CALIFORNIA UNIV LOS ANGELES DEPT OF PHYSICS

F/6 20/9

SIMULATION OF IONOSPHERIC EM-PLASMA INTERACTION IN A LARGE LABO--ETC(U)

JAN 81 A Y WONG, D L EGGLESTON

AFOSR-80-0012

UNCLASSIFIED

AFOSR-TR-81-0494

NL

1-1  
AD  
A100-007



END  
DATE  
FILMED  
FBI  
DTIC

UNCLASSIFIED

SECURITY CLASSIFICATION OF THIS PAGE (When Data Entered)

17 REPORT DOCUMENTATION PAGE		READ INSTRUCTIONS BEFORE COMPLETING FORM	
1. REPORT NUMBER <b>AFOSR-TR-81-0494</b>	2. GOVT ACCESSION NO. <b>AD-A100 007</b>	3. RECIPIENT'S CATALOG NUMBER <b>9</b>	
4. TITLE (and Subtitle) <b>SIMULATION OF IONOSPHERIC EM-PLASMA INTERACTION IN A LARGE LABORATORY DEVICE (Development of 2-D Cavitons)</b>		5. TYPE OF REPORT & PERIOD COVERED <b>Final</b> <b>15 Nov 79 - 15 Oct 80</b>	
7. AUTHOR(s) <b>A. Y. Wong D. L. Eggleston</b>		8. CONTRACT OR GRANT NUMBER(s) <b>AFOSR-80-0022</b>	
9. PERFORMING ORGANIZATION NAME AND ADDRESS <b>A. Y. Wong, Univeristy of California Department of Physics, 405 Hilgard Ave. Los Angeles, California 90024</b>		10. PROGRAM ELEMENT, PROJECT, TASK AREA & WORK UNIT NUMBERS <b>61102F 2301/A7</b>	
11. CONTROLLING OFFICE NAME AND ADDRESS <b>Air Force Office of Scientific Research/NP Bolling Air Force Base, Building 410 Washington, DC 20332</b>		12. REPORT DATE <b>Jan 1981</b>	
14. MONITORING AGENCY NAME & ADDRESS (if different from Controlling Office)		13. NUMBER OF PAGES <b>16</b>	
<b>LEVEL II</b>		15. SECURITY CLASS. (of this report) <b>Unclassified</b>	
		15a. DECLASSIFICATION/DOWNGRADING SCHEDULE	
16. DISTRIBUTION STATEMENT (of this Report) <b>Approved for Public release; distribution unlimited.</b>			
17. DISTRIBUTION STATEMENT (of the abstract entered in Block 20, if different from Report) <b>DTIC ELECT</b> <b>JUN 10 1981</b>			
18. SUPPLEMENTARY NOTES			
19. KEY WORDS (Continue on reverse side if necessary and identify by block number)  <b>Cavitons, Two-dimensional, electric fields, density profile modification.</b>			
20. ABSTRACT (Continue on reverse side if necessary and identify by block number) <b>Experimental observations of the time and space evolution of resonantly enhanced electric fields and plasma density in cylindrical geometry demonstrate the development of caviton structure in the direction perpendicular to the driving electric field. Electrostatic fields in this perpendicular direction are observed to have growth times on the ion time scale and to develop concurrently with two-dimensional density profile modification near the critical surface.</b>			

AD A100007

DTIC FILE COPY

DD FORM 1, 1473 EDITION OF 1 NOV 65 IS OBSOLETE

UNCLASSIFIED

SECURITY CLASSIFICATION OF THIS PAGE (When Data Entered)

Introduction

The interaction of electromagnetic (EM) waves with plasma is an area of research relevant to such diverse applications as laser-pellet fusion, RF/microwave heating of plasmas, and HF-induced ionospheric modification. In these applications one is interested in transforming the incident EM radiation into particle energy, thus heating the plasma. In a collisionless, unmagnetized, inhomogeneous plasma this transformation occurs in the following way<sup>9</sup>. Propagating EM waves with frequency  $\omega$  are reflected at the point where  $n = n_{\text{crit}} \cos^2 \theta$  where  $n_{\text{crit}}$  is the density where  $\omega = \omega_{pe}$ . At higher densities the wave is evanescent and the amplitude decays exponentially in space. For p-polarized EM waves (see Fig. 1) the component of  $\underline{E}$  parallel to the density gradient can drive an electrostatic resonance at  $n_{\text{crit}}$ . This electrostatic resonance gives rise to electron plasma waves which are then Landau damped, thus heating the electrons.

Since this process occurs near the critical density EM propagation effects in the subcritical plasma do not contribute to the physics of absorption. One can therefore simplify the experiment further by modeling the evanescent electric field between EM cutoff and the critical point with an electrostatic RF field -- the so-called capacitor plate type of experiment<sup>1,3</sup>.

Up until now, most microwave and capacitor plate investigations of critical surface phenomena have dealt only with phenomena in the dimension defined by the direction of the initial density gradient; the plasma density in the directions perpendicular to the density gradient was assumed to be uniform both initially and as the profile evolved. However, computer simulations (both fluid and kinetic)<sup>7</sup> and laser-plasma experiments<sup>8</sup> have indicated that two- and three-dimensional effects can play an important role in EM-plasma interactions.

81 6 10 023

Furthermore, 2-D numerical calculations on the evolution of Langmuir waves have shown that a 1-D soliton can, if perturbed, collapse in two and three dimensions<sup>5,6</sup>.

#### Summary of work performed

Stimulated by the above-mentioned results, we have performed experiments designed to investigate the two-dimensional evolution of an electrostatically driven inhomogeneous plasma. In pursuing this work we have

1. Developed a new cylindrically symmetric experimental device especially suited for a 2-D investigation.
2. Developed 2-D diagnostics which allow us to measure phenomena anywhere on the 2-D plane.
3. Set up a computerized data taking system to efficiently handle the great volume of data involved in a 2-D investigation.
4. Made the first observation of the development of two-dimensional structure in cavitons. These observations, which have been submitted for publication, are described in detail in the next section.
5. Developed a simple theoretical model based on previous 1-D work<sup>2</sup> to explain our results.

Accession/For	
NTIS GRA&I	
DTIC TAB	
Unannounced	
Justification	
By	
Distribution/	
Availability	
Dist	Avail an Special
A	

#### Development of Two-Dimensional Structure in Cavitons

The experiment was performed in the cylindrically symmetric device shown in Figure 2. A weakly ionized Argon plasma ( $n_e \approx 10^9 \text{ cm}^{-3}$ ,  $P_n = 2 \times 10^{-4} \text{ torr}$ ) was produced by a pulsed HF oscillator ( $\nu = 10 \text{ MHz}$ , pulse length =  $25 \mu\text{s}$ , duty cycle < 25%) connected to a long, cylindrical antenna consisting of twelve rods extending axially and equally spaced azimuthally. The experiment is performed in the quiescent discharge afterglow where  $\delta n/n < 0.3\%$ ,  $T_e = 1.0 \text{ eV}$ ,  $T_i = 0.1 \text{ eV}$ ,

AIR FORCE OFFICE OF SCIENTIFIC RESEARCH (AFSC)

NOTICE OF TRANSMITTAL TO DDC

This technical report has been reviewed and is approved for public release IAW AFR 190-12 (7b). Distribution is unlimited.

A. D. BLOSE

Technical Information Officer

and  $\lambda_D = 0.23$  mm. The density gradient in the experimental region is primarily in the radial direction [ $L = \left( \frac{1}{n_0} \frac{\partial n}{\partial r} \right)^{-1} = 16$  cm] and the coaxial line formed by the central rod and the chamber wall provides a purely radial quasistatic driving field ( $\nu_0 = 285$  MHz,  $P < 100$  watts,  $E_{vac} < 4$  V/cm typically) to produce the caviton. This is in contrast to the 1-D capacitor plate experiments<sup>1</sup> where fringing driver fields in the direction perpendicular to the density gradient are unavoidable. The cylindrical geometry also allows one of the directions perpendicular to the density gradient to close on itself, thus avoiding boundary effects.

The caviton electric field is measured with an unperturbing diagnostic electron beam<sup>1,4</sup> ( $\phi_b = 7.5 - 9.0$  kV,  $I_b = 0.1$   $\mu$ A) with a temporal (spatial) resolution of 0.2  $\mu$ s (1 mm). The beam can be mechanically moved both radially and azimuthally which allows us to diagnose the entire  $r, \theta$  - plane. The plasma density is measured with a small wire probe (10 mil. diameter, 0.2" long) positioned by a two-dimensional probe drive. Movement of the probe is controlled by a computer which also stores the data on flexible magnetic disks. Time resolution is obtained through the use of a boxcar averager.

The basic experimental sequence is as follows: at a selected time in the discharge afterglow a short (1 - 10  $\mu$ s) VHF burst ( $P < 100$  watts) is applied to the center electrode of the chamber to drive the caviton. At a selected time  $t$  within the VHF burst a shorter ( $< 1$   $\mu$ s) voltage pulse is applied to the electron gun. The caviton-modulated image of this electron burst is then measured on the phosphorus screens at a selected coordinate ( $r, \theta$ ). Only fields greater than 4 V/cm produce an observable modulation thus making this diagnostic sensitive to resonantly-enhanced fields ( $E \sim 100$  V/cm) but not to the driver field ( $E < 4$  V/cm). After measuring the axial dependence of the caviton one can unfold this image data to get the amplitude, direction, and relative

phase of the enhanced VHF electric field at  $(r, \theta, t)$ . When density data are taken, the probe current is sampled approximately 2  $\mu\text{s}$  after the end of the VHF burst to avoid spurious probe effects.

In previous experiments<sup>1</sup> the caviton electric field was always in the same direction as the driving field. Such a response is shown in Fig. 2b where the caviton field is purely radial and has a shape characterized by a large resonance and several smaller subcritical peaks; this shape is quite similar to the Airy function solution of the so-called capacitor plate problem<sup>2</sup>. The plasma density response to the ponderomotive force of the field is shown in Fig. 2c. Our main new finding is that this caviton can evolve in such a way as to produce a strong electric field component in the direction perpendicular to the driving field.

Figures 3a, b, c, show the magnitude, direction, and relative phase of the electric field at time  $t = 0.5 \mu\text{s} = 3.3 \omega_{pi}^{-1}$  for a section of the polar plane. Note that at this early time in the VHF burst the enhanced electric field is purely radial and that it has very little azimuthal dependence. Two-dimensional density measurements show that the initial (zeroth-order) density has good symmetry and has no strong gradients in the azimuthal direction. Thus initially we have a fairly symmetric caviton that forms a ring concentric with the center conductor and has purely radial electric fields.

Figures 3d, e, f show the same polar section at a later time in the VHF burst ( $t = 6.75 \mu\text{s} = 44.6 \omega_{pi}^{-1}$ ). The electric field magnitude has now developed an azimuthal dependence thus destroying the initial azimuthal symmetry. The field has also developed a vector component in the  $\theta$ -direction that is comparable in magnitude to the radial component. More detailed temporal measurements show that the growth and decay time for  $|E_\theta|$  is  $\sim 1.5 \mu\text{s} = 10 \omega_{pi}^{-1}$ . As indicated by the Lissajous patterns in Fig. 3e, there is a definite, spatially

varying phase relationship between the  $E_r$  and  $E_\theta$  components of the measured electric field.

Two-dimensional plasma density measurements are shown in Figure 4. Experimental conditions are similar to those existing during electric field measurements. The critical density occurs at  $r \approx 8$  cm and consecutive contours correspond to a density change of  $\frac{\delta n}{n_{\text{crit}}} \approx 1.26\%$ . Note that a larger polar section is shown here than in Figure 3. Figure 4a shows the zeroth order (undriven) density which decreases with increasing  $r$  and is fairly symmetric azimuthally. The density ripples at large  $r$  are due to the regularly spaced rods of the plasma production antenna. At the critical surface the magnitude of these ripples is  $\frac{\delta n}{n} \approx 0.5\%$  with an azimuthal wavelength of  $\lambda = 4.1$  cm  $= 180 \lambda_D$ .

Figures 4b and 4c show isodensity contour plots taken after a 1  $\mu$ s and 8  $\mu$ s VHF burst, respectively. Dotted contours indicate a closed contour which contains a local minimum (density hole). As with the electric field measurements, we again see an increase in the azimuthal asymmetry with VHF burst length. In Figure 4c radially and azimuthally localized density structures have developed. Note that the azimuthal spacing of these structures ( $\Delta\theta \approx 30^\circ$ ) matches the azimuthal peak-to-peak spacing of the enhanced electric field (Fig. 3d, f). Further, note that the azimuthal locations of these density structures correspond to the density minima of the perturbation caused by the rods of the plasma production antenna.

A simple model to explain the development of two-dimensional structure from an initial perturbation is as follows. Consider a linear density profile with a periodic perturbation in both the density and the density gradient scale length  $L = n_0 (\partial n / \partial x)^{-1}$ :

$$n(x, y) = n_0 (1 + x/L(y) + \epsilon \cos ky) \quad (1)$$

where  $n_0$  is the critical density and  $L(y) = L_0 (1 + \epsilon \cos ky)^{-1}$ . Here  $x$  is the

direction of the driving electric field (corresponding to our  $r$ ) and  $y$  is perpendicular to the driver (our  $\theta$ ). Adopting the scaling of Morales and Lee<sup>2</sup>, the solution for  $E_x$  when  $\partial E_x / \partial x \gg \partial E_x / \partial y$  is  $E_x(x, y) = (k_D L)^{2/3} E_0 A(\eta, t)$  where  $\eta = (k_D L)^{2/3} (x/L + \epsilon \cos ky)$ ,  $k_D = (\text{Debye length})^{-1}$ ,  $E_0$  is the driver field, and  $A$  is the spatial variation of the enhanced electric field and has amplitude of order one. Using the electrostatic condition,  $\partial E_x / \partial y = \partial E_y / \partial x$ , and integrating over  $x$  one can solve for  $E_y$ . Near the critical surface and to first order in  $\epsilon$  we obtain:

$$E_y(x, y) = - (L_0 \epsilon k \sin ky) E_x(x, y) \quad (2)$$

The critical surface with nonlinear perturbation is now defined by  $x/L + \epsilon \cos ky + \delta n/n_0 = 0$  where  $\delta n/n_0 = -E^2/16\pi n_0 T_e$  and  $E^2 = E_x^2 + E_y^2$ . We can rewrite this as  $\eta = \gamma P(y) A^2(\eta, t)$  where  $\gamma = (k_D L_0 E_0)^2/16\pi n_0 T_e$ ,  $P(y) = (1 + \delta \sin^2 ky)/(1 + \epsilon \cos ky)^2$ , and  $\delta = (L_0 \epsilon k)^2$ . We must, in general, solve this transcendental equation for  $\eta$  for each value of  $y$ . However, since our perturbation is small  $P(y) \approx 1$  and we can expand  $A^2(\eta, t)$  around the value  $\eta_0 = \gamma A^2(\eta_0, t)$ . Keeping terms of first order in  $\epsilon$  and  $\delta$  we obtain for the modified profile near the critical surface:

$$n(x, y) \approx n_0 \left\{ 1 - \mu + x/L(y) + [1 + \mu(4/3 + 2\beta)] \epsilon \cos ky - \mu(1 + \beta) \delta \sin^2 ky \right\} \quad (3)$$

where  $\beta = 2\eta_0 A'(\eta_0, t)/[A(\eta_0, t) - 2\eta_0 A'(\eta_0, t)]$  and  $\mu = \eta_0/(k_D L_0)^{2/3}$ . If we choose for  $A(\eta, t)$  the steady state Airy function solution<sup>2</sup> it can be shown that for all positive  $\eta_0$ ,  $-0.2 \leq \beta \leq 0$ . Then comparing equations (1) and (3) one can see that the nonlinear modification to the density near the critical surface has increased the amplitude of the density perturbation. In addition, second harmonics of the initial perturbation are produced by the  $\sin^2 ky$  term



which represents the beginning of localization in the  $y$ -direction. Thus this approximate model suggests a mechanism for the production of an  $E_y$  electric field component with a spatially varying phase relationship to  $E_x$  and for the non-linear development of two-dimensional density structure from an initial perturbation.

Our observations are also reminiscent of theoretical studies<sup>5</sup> of soliton collapse in two-dimensions. Ongoing theoretical work<sup>6</sup> has shown that a similar collapse can occur in an inhomogeneous, externally driven plasma. More detailed measurements of the structure growth rates and the trapping of VHF fields should reveal which model(s) should be used to explain our data. Our work may also be relevant in explaining the small scale rippling of the critical surface as observed in laser-plasma simulations and experiments<sup>7</sup>, although such rippling is usually attributed to electromagnetic effects.

REFERENCES

1. H. C. Kim, R. L. Stenzel, and A. Y. Wong, Phys. Rev. Lett. 33, 886 (1974);  
P. DeNeef, Phys. Rev. Lett. 39, 997 (1977);  
A. Y. Wong, P. Leung, D. Eggleston, Phys. Rev. Lett. 39, 1407 (1977).
2. G. J. Morales and Y. C. Lee, Phys. Fluids 20, 1135 (1977).
3. D. L. Eggleston, A. Y. Wong, and C. B. Darrow, Bull. Am. Phys. Soc. 25, 1036 (1980).
4. R. S. Harp, W. B. Cannara, F. W. Crawford and G. S. Kino, Rev. Sci. Instrum. 36, 960 (1965).
5. N. R. Pereira, R. N. Sudan, and J. Denavit, Phys. Fluids 20, 936 (1977);  
D. R. Nicholson and M. V. Goldman, Phys. Fluids 21, 1766 (1978).
6. N. R. Pereira and G. J. Morales, UCLA Plasma Physics Report, PPG-529.
7. K. Estabrook, Phys. Fluids 19, 1733 (1976);  
K. Estabrook, E. J. Valeo, and W. L. Druet, Phys. Fl. 18, 1151 (1975);  
E. J. Valeo and K. G. Estabrook, Phys. Rev. Lett. 34, 1008 (1975);  
E. L. Lindman, J. Physique, Colloque C6, 9 (1977);  
K. Estabrook, Phys. Rev. Lett. 41, 1808 (1978);  
C. Randall and J. S. DeGroot, Phys. Rev. Lett. 42, 179 (1979).
8. R. S. Craxton and M. G. Haines, Phys. Rev. Lett. 35, 1336 (1975);  
K. R. Maines, H. G. Ahlstrom, R. A. Haas, and J. F. Holzrichter, J. Opt. Soc. Am. 67, 717 (1977);  
Y. Sakigami, H. Kawakami, S. Nagas, C. Yamanaka, Phys. Rev. Lett. 42, 839 (1979);  
N. M. Ceglio and J. T. Larsen, Phys. Rev. Lett. 44, 579 (1980).  
H. Nishimura et al., Pl. Phys. 21, 69 (1980).

9. A. Y. Wong, "Electromagnetic Wave Interactions with Inhomogeneous Plasmas",  
in Laser Interactions and Related Phenomena, Vol. 4B, 1977;  
A. Y. Wong and R. L. Stenzel, Phys. Rev. Lett. 34, 727 (1975).

Figure Captions

- Figure 1. Schematic drawing of the propagation of a p-polarized electromagnetic wave in an inhomogeneous plasma.
- Figure 2a. Schematic diagram of the experimental apparatus showing coaxial experimental area on right and movable diagnostic beam on left.
- Figure 2b. Cavity field amplitude vs. radial position at  $t = 0.5 \mu s$  and azimuthal position  $\theta = 90^\circ$  ( $0^\circ$  being top of chamber and increasing clockwise facing phosphor windows). Enhanced fields at inner conjugate resonance point ( $r \approx 3 \text{ cm}$ ) are outside the range of the electron beam diagnostic.
- Figure 2c. Electron density profile corresponding to field profile in Fig. 1b.
- Figure 3a. Contour plot of cavity E-field amplitude at  $t = 0.5 \mu s$  for a section of the polar plane. Contour level is proportional to field amplitude and level changes by 6 V/cm with each line. Minimum and maximum values are zero and 144 V/cm respectively.
- Figure 3b. Equal length arrow plot for  $t = 0.5 \mu s$ . Direction of arrow gives direction of electric field.
- Figure 3c. Three dimension graph of the same data as in 2a. Third dimension is proportional to  $|E|$ .
- Figure 3d. Contour plot of total cavity electric field at  $t = 6.75 \mu s$  for same polar section. Contour level changes by 3 V/cm with each line. Minimum and maximum values are zero and 85.5 V/cm respectively.
- Figure 3e. Equal length arrow plot for  $t = 6.75 \mu s$ . Relative size of  $E_r$  and  $E_\theta$  can be determined from inclination of arrow and relative phase can be determined from arrow direction. When relative

phase was  $90^\circ$  an ellipse was drawn with (major axis)/(minor axis) =  $|E_r|/|E_\theta|$ .

Figure 3f. Three dimensional graph of the same data as in 2d.

Figure 4. Isodensity contour plots a) before the VHF burst, b) after a  $1 \mu\text{s}$  VHF burst, and 3) after a  $8 \mu\text{s}$  VHF burst.

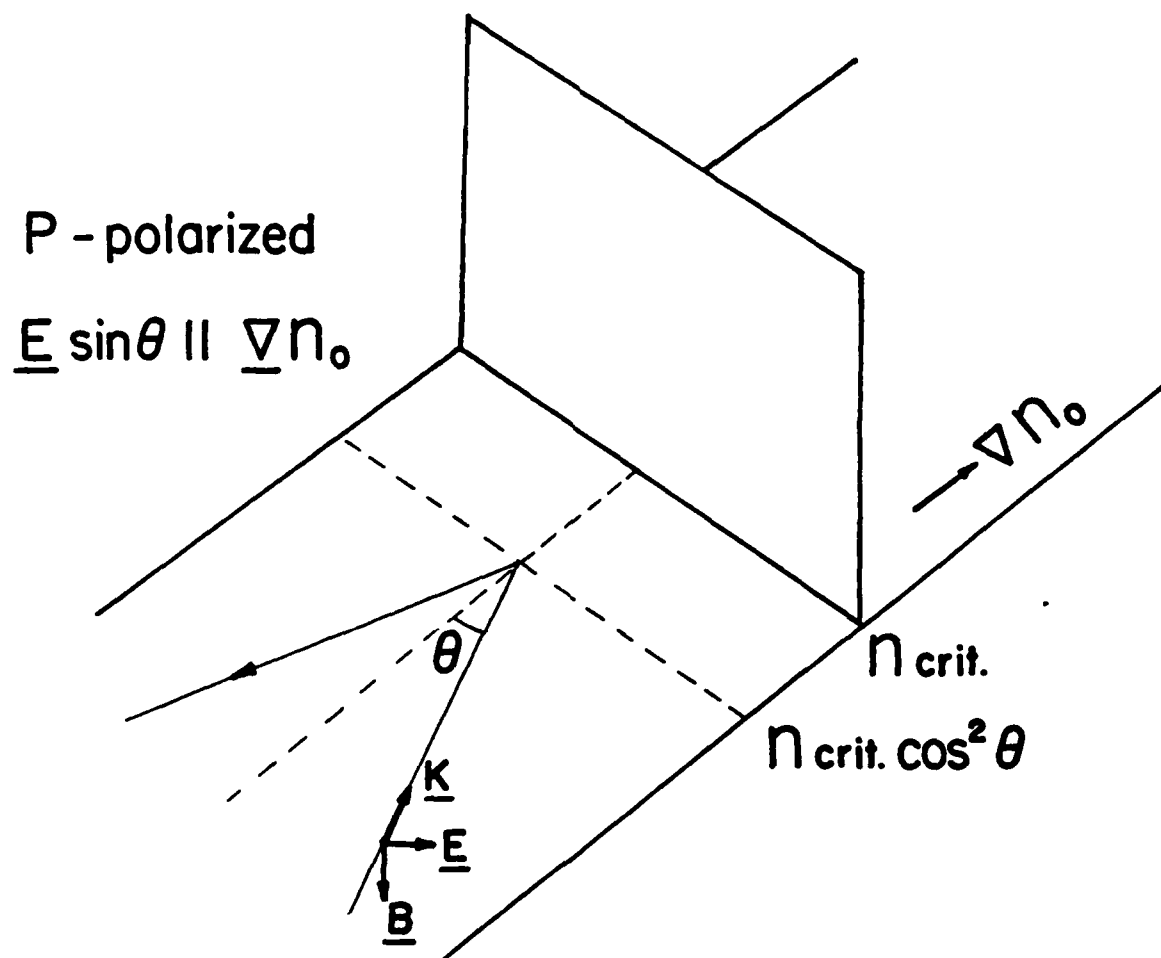


Figure 1

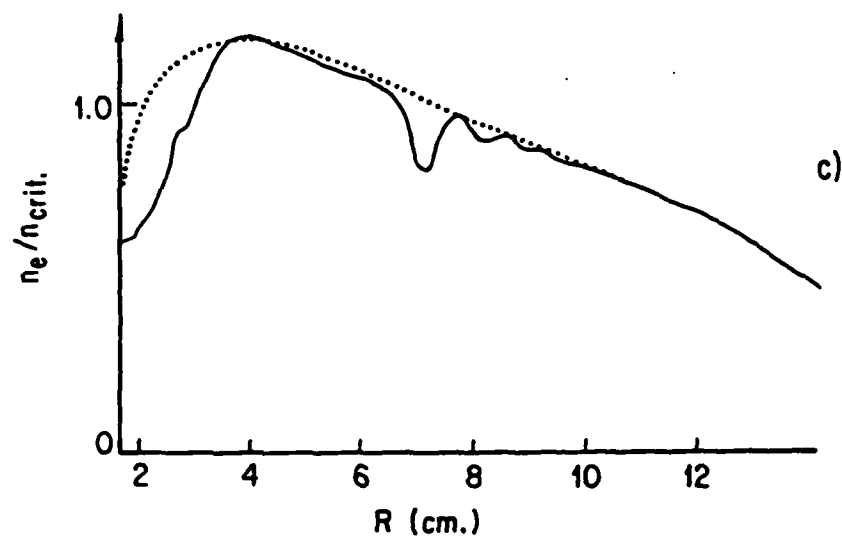
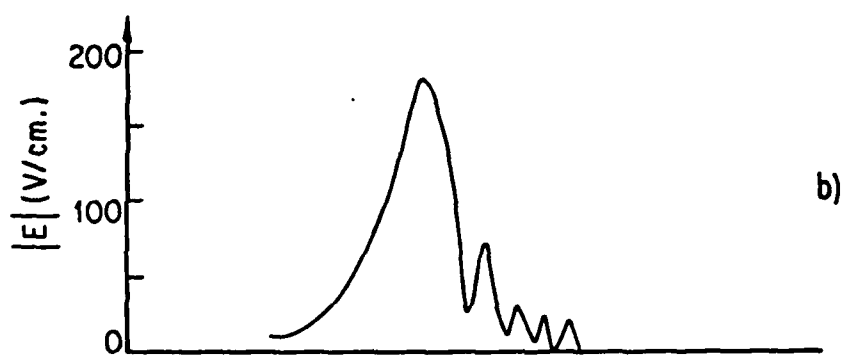
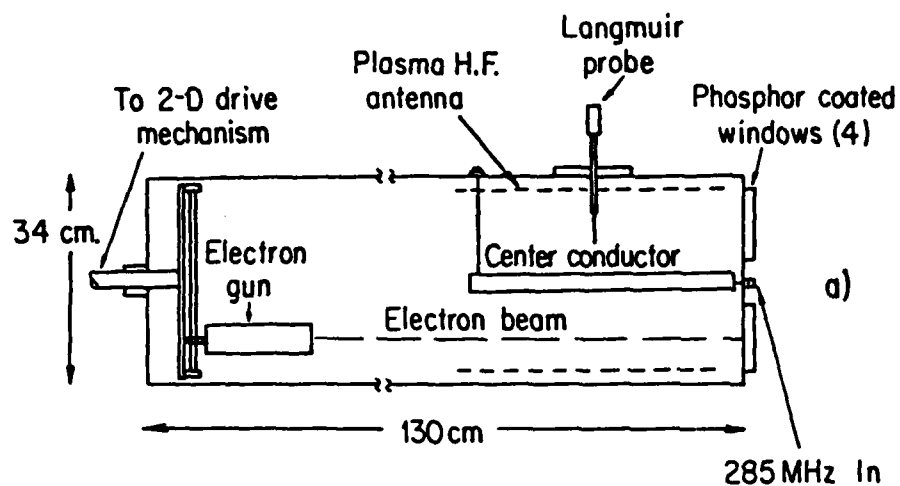


Figure 2

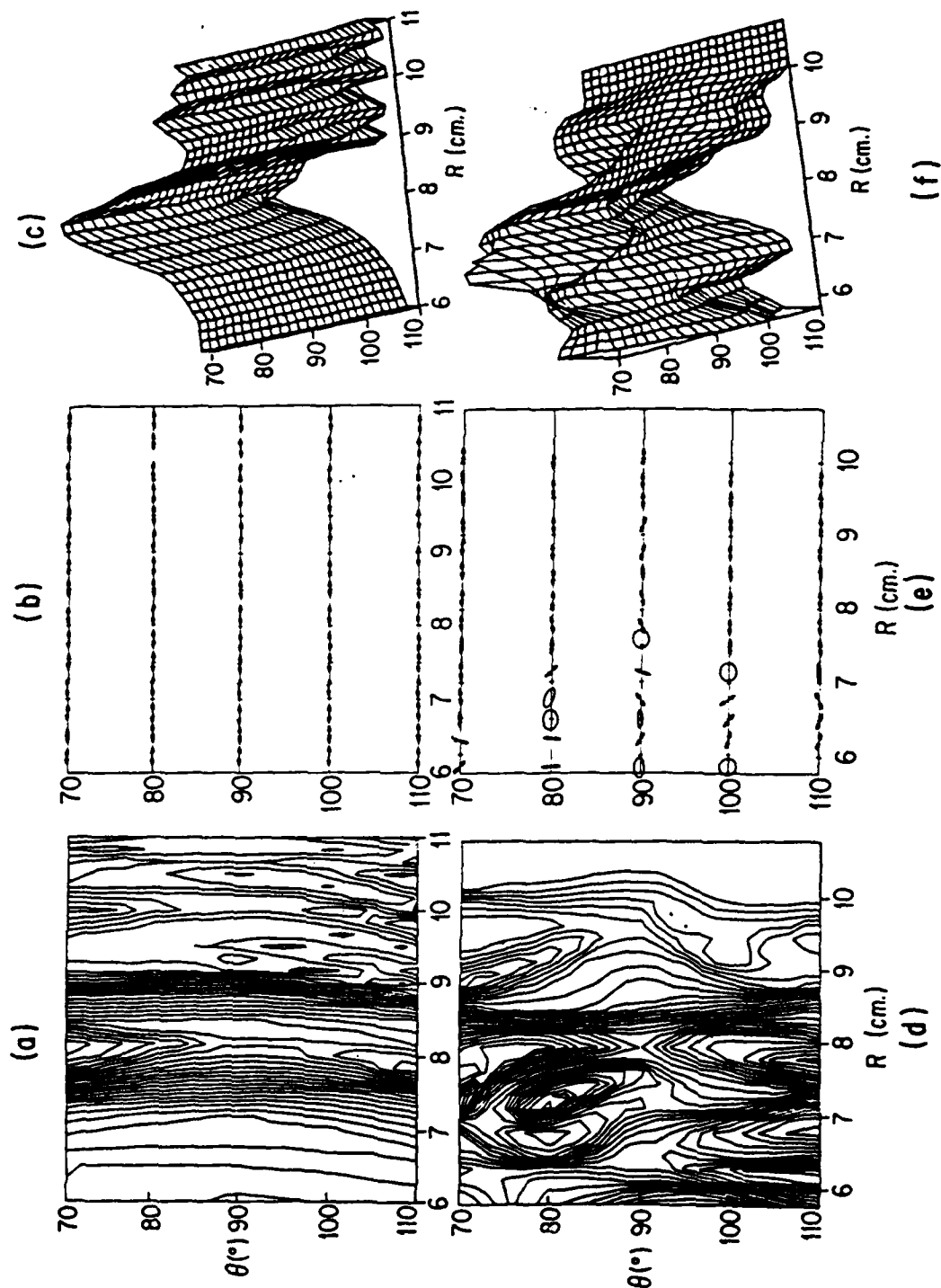


Figure 3



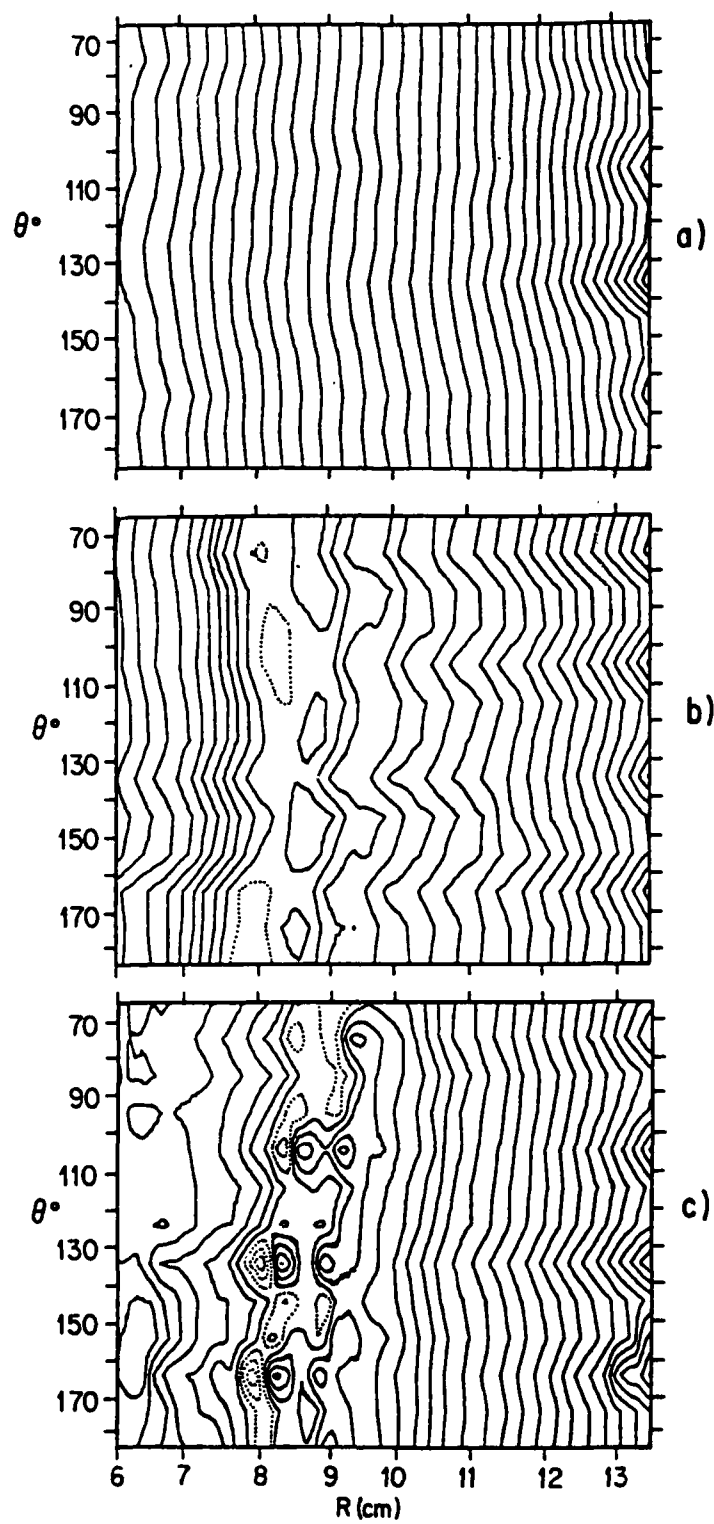


Figure 4

The following is the title and abstract of our work performed under  
[REDACTED] which was presented at the American Physical Society  
*AFOSR-80-0012*  
Meeting, San Diego, California, November 10-14, 1980.

9T 20 Development of Two-Dimensional Structure in Cav-  
itons.\* D. L. EGGLESTON, A. Y. WONG, C. B. DARROW, UCLA.  
--A coaxial capacitor plate experiment in which the dri-  
ving field and the density gradient are both in the rad-  
ial direction only is performed to study RF-plasma inter-  
actions in two dimensions ( $\nu = 285$  MHz).<sup>1</sup> The time and  
space evolution of resonantly enhanced electric fields  
and plasma density are measured in two-dimensions by a  
non-perturbing scanning diagnostic electron beam and a  
thin wire probe, respectively. These measurements dem-  
onstrate the development of caviton structure in the di-  
rection perpendicular to the driving electric field.  
Electrostatic fields in this perpendicular direction are  
observed to develop concurrently with density profile  
modification and critical surface rippling and have  
growth times on the ion time scale. Possible mechanisms  
for this two-dimensional evolution are considered.

\*Work supported by AFOSR Grant 80-0012.

<sup>1</sup>D. L. Eggleston, C. B. Darrow and A. Y. Wong, Bull.  
APS 24, 959 (1979).

This work has been reported in UCLA Plasma Physics Group Report #506  
and has been submitted to Physical Review Letters for publication.